Thermo-kinetic behaviour of green synthesised nanomaterial enhanced organic phase change material: Model fitting approach

Abstract: Metal, carbon and conducting polymer nanoparticles are blended with organic phase change materials (PCMs) to enhance the thermal conductivity, heat storage ability, thermal stability and optical property. However, the existing nanoparticle are expensive and need to be handle with high caution during operation as well during disposal owing to its toxicity. Subsequently handling of solid waste and the disposal of organic PCM after longevity usage are of utmost concern and are less exposed. Henceforth, the current research presents a new dimension of exploration by green synthesized nanoparticles from a thorny shrub of an invasive weed named Prosopis Juliflora (PJ) which is a agro based solid waste. Subsequently, the research is indented to decide the concentration of green synthesised nanoparticle for effective heat transfer rate of organic PCM (T_m=35-40°C & H_m=145 J/g). Furthermore, an in-depth understanding on the kinetic and thermodynamic profile of degradation mechanism involved in disposal of PCM after usage via Coats and Redfern technique is exhibited. Engaging a two-step method, we fuse the green synthesized nanomaterial with PCM to obtain nanocomposite PCM. On experimental evaluation, thermal conductivity of the developed nanocomposite (PCM+PJ) increases by 63.8% (0.282 W/m·K to 0.462 W/m·K) with 0.8 wt% green synthesized nanomaterial owing to the uniform distribution of nanoparticle within PCM matrix thereby contributing to bridging thermal networks. Subsequently, PCM and PCM+PJ nanocomposites are tested using thermogravimetric analyzer at different heating rates (05°C/min; 10°C/min; 15°C/min & 20°C/min) to analyze the decomposition kinetic reaction. The kinetic and thermodynamic profile of degradation mechanism involved in disposal of PCM and its nanocomposite of PCM+PJ provides insight on thermal parameters to be considered on large scale operation and to understand the complex nature of the chemical reactions. Adopting thirteen different chemical mechanism model under Coats and Redfern method we determine the reaction mechanism; kinetic parameter like activation energy (Ea) & pre-exponential factor (A) and thermodynamic parameter like change in enthalpy (ΔH), change in Gibbs free energy (ΔG) and change in entropy (ΔS). Dispersion of PJ nanomaterial with PCM reduces Ea from 370.82 kJ/mol^{-1} to 342.54 kJ/mol^{-1} (7.7% reduction), as the developed nanomaterial is enriched in carbon element and exhibits a catalytic effect for breakdown reaction. Corresponding, value of ΔG for PCM and PCM+PJ sample within heating rates of 05-20°C/min varies between 168.95-41.611 kJ/mol^{-1}. The current research will unbolt new works with focus on exploring the pyrolysis behaviour of phase change materials and its nanocomposite used for energy storage applications. This work also provides insights on the disposal of PCM which is an organic solid waste. The thermo-kinetic profile will help to investigate and

predict the optimum heating rate and temperature range for conversion of micro-scale pyrolysis to commercial scale process.

Keywords: Thermal Energy Storage; Phase Change Material; Sustainable Nanomaterial; Thermal Decomposition Kinetics; Coats and Redfern method; Disposal

1.0 Introduction

Over the past decades, phase change materials (PCMs) are efficiently researched, tested, commercialized and actively used for thermal comfort of buildings (Naveenkumar et al. 2022), solar thermal system & desalination units (Boopalan et al. 2021, Balal et al. 2023), building heating and cooling (Tyagi et al. 2021), battery thermal management (Subramanian et al. 2021, Oyewola, Awonusi and Ismail 2022) and also with electronic gadgets because of high latent heat, non-flammability, ease in availability and low cost. So, the current research scope is an active thermal energy storage unit trapping the solar energy and supplying it for thermal regulations. PCMs are actively used as thermal batteries for storing solar power during day time and it actively discharges the solar power during inconsistent period for effective usage but still there are some challenges such as poor thermal conductivity which can limits their heat transfer rate and their response time.

1.1 Need for the Current Art-of-Research

Phase change materials are generally classified into three a) organic materials (paraffin and esters), b) inorganic materials (salt hydrates), and c) eutectic materials (blends of organic-organic | organic-inorganic | inorganic-inorganic) (Kalidasan et al. 2022b). Organic PCMs are selected for long-term operation and energy storage system owing to their stability and low toxicity, however they thermal conductivity, uneven temperature distribution and poor heat removal. Numerous research works has been conducted by dispersing metal nanoparticle, metal foam, carbon nanoparticle (single walled carbon nanotube; multi-walled carbon nanotube (Atinafu et al. 2021); graphene; reduced graphene; expanded graphite; expanded perlite and tetrapods) (Balasubramanian et al. 2023), unique dimensioned nanomaterials to enhance the thermal features of the PCMs. All the listed nanomaterials do increase the thermal conductivity of the PCM matrix significantly. However, all the aforementioned nanomaterials continue to confront challenges with high manufacturing costs and toxic in nature. In addition, after usage, these nanoparticles are eventually dispersed into the environment, henceforth there is an utmost need for eco-friendly nanoparticles. New dimensions of exploration using green synthesize nanoparticles are of interesting research domain. Green synthesized nanomaterial are a new environmental friendly safer material; and can be prepared from agro & forest residues (Hagemann et al. 2018) with other superior benefits as a) cheaper; b)

renewable; c) ease of preparation; d) large sorption potential; e) protect environment as can be developed from waste and e) high surface area (Magnacca et al. 2018). Whereas in the current research we perform carbonizing in a controlled atmosphere ensuring pollution free synthesis technique. Furthermore, there is an utmost attraction towards synthesis of eco-friendly nanomaterials demonstrating effective thermo-physical characteristics to compete with the commercial nanomaterials.

Subsequently, the quantity of phase change material indent for any application is huge based on the latent heat potential and it needs a reliable technique for its disposal after usage. Though phase change materials are not harmful they fall under the category of hydrocarbons as persistent organic pollutant (POPs) as far as its disposal is concerned. Based on, the environmental policies from, Department of Environment Ministry of Natural Resources, Environment and Climate Change, Malaysia, there are predefined technical guidelines (Annex) for environmentally sound management of waste consisting of contaminated with (POP)s, and the same is applicable for most of the ASEAN nations. The guidelines state pre-treatment of the material adopting any of the methods like a) dewatering, b) size reduction, c) mechanical separation, d) thermal desorption, e) adsorption and absorption, f) pH adjustment and g) oil-water separation before being adopting disposal techniques like hazardous-waste incineration, plasma arc, waste to gas conversion etc. Henceforth it is important to explore a pre-treatment and degradation technique that assist ease of disposal of the used phase change material which is generated as solid waste material. Based on the above discussed problems the current art of research is indented to a) develop a green synthesis nanomaterial using weed shrubs of Prosopis Juliflora (PJ), b) to develop a nanocomposite PCM using polyethylene glycol and the green synthesised PJ biochar based nanomaterials at different weight proportions and c) exhibit the degradation mechanism that assist pretreatment as well as ease of disposal of the developed nanocomposite PCM.

1.2 Literature Works

Numerous research works on biochar preparation and their utilization with energy storage domains were explored. Zhang et al. (Zhang et al. 2019) conducted an experimental investigation by using carbonized corn as a supporting material to resolve leakage issues of binary eutectic of lauric-stearic acid. Results depict that leakage issue was completely resolved with 77.9 wt% of binary eutectic PCM with 22.1 wt% of corn cob for nano composite PCM. Sheng et al. (Sheng et al. 2020) dispersed biochar derived from sisal fibre (1D carbon bundles) with paraffin to enhance the thermal conductivity from 0.25 W/m·K to 1.73 W/m·K at carbon ratio of 12.8%. Significant improvement in thermal conductivity of the composite was attributed by the anisotropic one dimensional arrangement

of sisal fibres exhibited better thermal networks. Likewise, Das et al. (Das et al. 2020) dispersed biochar of water hyacinth (PCM: biochar of 4:6; 5:5; 6:4; 7:3; 8:2; 9:1 wt%) to develop form stable PCM with improved thermal conductivity of composite PCM by 13.8 times (PCM: biochar of 6:4 wt%). In another research work, Atinafu et al. (Atinafu et al. 2021) developed a hybrid nanoparticle combining MWCNT with biochar of bamboo for efficient encapsulation of PCM. Pristine bamboo biochar depicted low latent heat and PCM loading ratio, in comparison with hybrid MWCNT-bamboo biochar owing to the lower pore space, and robust intermolecular attraction between PCM and the function groups. Hekimoglu et al. (Hekimoğlu et al. 2021) conducted an experimental investigation using biochar of walnut shell with methyl palmitate for improving the thermal energy storage. A comparison between biochar of walnut shell and activated biochar of walnut shell shows an increase in pore volume and surface area of the bio carbons by 1.44 and 1.47 times respectively. Higher surface area and pore volume enhanced the fusion enthalpy of activated biochar walnut shell based PCM than normal walnut shell biochar PCM. Goud et al. (Goud and Raval 2022) used 24% of neem wood based biochar material with 76% of paraffin to enhance the thermal energy storage enthalpy and shape stability of the PCM for battery thermal management. Likewise, Lv et al. (Lv et al. 2022) experimentally investigated the thermal performance of a variety of PCM like paraffin, stearic acid and PEG using biochar developed from phoenix leaf. The PCM:biochar proportion was 75:25 wt%. Interestingly, results depicted that biochar pyrolyzed at higher temperature caused higher graphitization and increased the thermal conductivity of nanocomposites, rather than the biochar nanoparticle pyrolyzed at lower temperature. Mandal et al. (Mandal et al. 2022) used pinus resinosa biochar material as supporting material with dodecanoic acid as PCM. Xiong et al. (Xiong et al. 2022) in his research used garlic stem biobased nanoparticle to enhance the thermal performance of paraffin wax. Bordoloi et al. (Bordoloi et al. 2022) used sugarcane bagasse waste to prepare supporting matrix for organic PCM. Likewise Chen et al. (Chen et al. 2023) developed bio nanoparticle using a hybrid source of corn straw and graphene oxide to supper the leakage issue of organic PCM. Zhang et al. Conversely, as of now, most of the experimental works report utilization of biochar material as a supporting material for shape stabilized PCMs and form stable PCM.

As well on the other perspective, after repeated usage the PCM and its nanocomposite is of excess organic solid waste and its disposal seeks great attention (Kalidasan et al. 2023a). The decomposition kinetics of the developed nanocomposite is explored by pyrolysis technique under the absence of oxygen. Treating the used nanocomposite PCM via pyrolysis technique would enhance the sustainability of PCM as this would lead to extract the end used nanocomposite PCM to be converted as renewable fuels and byproducts. Pyrolysis is a low energy demanding method and more eco-friendly technique in comparison with combustion and gasification. To explore this technique at

industrial level, there requires an elaborative mechanism investigation of nanocomposite PCM decomposition in terms of pyrolytic performance, thermal degradation, kinetic and thermodynamics factors. De Jesus (de Jesus et al. 2019) conducted a thermal behavior of wood using macro-thermogravimetric analysis to explore the rate of decomposition and energy peak. Yousef et al. (Yousef et al. 2021) investigated the kinetic behavior of the decomposition of glass fiber thermoplastic to identify the elemental composition of volatile materials and activation energy based on existing linear and non-linear models. El-Sayed et al. (El-Sayed, Khass and Mostafa 2023) used variety of biomass (palm fronds, olive leaves and wheat straw) to evaluate the chemical kinetic behavior using TGA. In another work, pyrolysis analyses of camel manure was conducted at varying heating rates of 10 K/min, 20 K/min and 50 K/min at N_2 inert atmosphere (Al-Rumaihi et al. 2021). Likewise, Ming et al. (Ming et al. 2020) conducted thermal degradation analysis of food waste (Rice & Pork) using TG-FTIR and exhibited the values of change in enthalpy, entropy and Gibbs free energy to support the complexity of pyrolysis process of different food type. In the peak of COVID-19, major medical solid waste was the used masks, Nawaz et al. (Nawaz and Kumar 2022) conducted a thermal degradation analyses of three layer mask by incorporating artificial neural network predicting model. Kottala et al. (Kottala et al. 2023) explored the thermal decomposition kinetics of D-Mannitol a family of sugar alcohol PCM in addition to chemical and thermal characterization. D-Mannitol was interspersed with multi wall CNT for enhancing the thermal conductivity. In his research work, model free kinetic techniques like Flynn Wall Ozawa, Kissinger Akahira Sunose, and Starink were used to determine the activation energy and thermodynamic parameters.

1.3 Novelty of the Current Research

Policymakers and industries at present are exploring technology and processes for converting waste material into products with added value. Prosopis Juliflora (PJ) a family of Fabaceae, as a thorny shrub of about 3-5 m or a small tree at a height of 15 m; in an invasive weed with a uniqueness of roots to penetrate deeper in search of ground water being scary to the native biodiverse plants (Keeran et al. 2019). In addition, it is abundantly available in Africa, Asia, Australia and South America, esteemed to be used as fuel source, timber and also as soil erosion control. Henceforth, we develop nanoparticles from agro waste and try to commercialize them. Kinetic and thermal parameters are necessary for the design, operation, and optimization of the scale-up system (Açıkalın 2022). Several researchers have studied the decomposition kinetics of solid agro-waste as discussed in the literature using thermogravimetric analysis in estimating kinetic parameters of such complex processes (Balasubramanian et al. 2022, Karaeva et al. 2022). Nonetheless, there is no existing work reporting green synthesis of nanomaterials using weed shrubs of Prosopis Juliflora (PJ) and its byproducts. These PJ plants are invasive weed shrubs as their roots are well arranged in a way to penetrate deeper

in search of ground water, thereby being scary to the native biodiverse plants, and are widely used as solid fuels in Asia and Africa. Transformation of such scary weed plant solid waste into useful nanomaterial for enhancing the thermal characteristics of energy storage materials is of utmost benefit. Furthermore, exploring the thermal degradation kinetics and thermodynamic factor involved in decomposition of organic PCM and its nanocomposite specifically with green synthesized nanomaterial derived from shrubs of Prosopis Juliflora is state of the art. Based on literature, there exist a need for a more eco-friendly and economically viable nanoparticle, as an effective solution to overcome the low thermal conductivity issue of phase change materials. Eventually, the current experimental research investigation aims to develop an eco-friendly green synthesized nanomaterial using the roots and branches of waste weed plant Prosopis Juliflora. As a beneficial note, the weed shrubs of PJ exhibit higher surface area ratio owing to their micro-pores enabling better intermolecular attraction. The green synthesized PJ nanomaterial is dispersed within the matrix organic PCM PEG-1000 operating at a temperature range of 38°C for enhancing the thermal characteristics. The thermal conductivity of organic PCM PEG-1000 is enhanced from 0.282 W/m·K to 0.462 W/m·K overall contributing to 63.8% increment. Despite, the research exploits the decomposition behaviour of the green synthesized PJ based nanocomposite and base PCM using thermogravimetric analyzer (TGA) at different heating rates of 5°C/min, 10°C/min, 15°C/min and 20°C/min we adopt a co-pyrolysis and co-combustion technique to express thermo kinetic profile. Using the TGA curve data's reactivity analysis of the PCM and its nanocomposite with PJ nanomaterials is compared and elaborated. Thirteen models based on Coats-Redfern technique were numerically followed to evaluate the kinetic [activation energy (E_a) & pre-exponential factor (A)] and thermodynamic [change in enthalpy (ΔH), change in Gibbs free energy (ΔG) and change in entropy (ΔS)] parameters. The current research will unbolt new works with focus on exploring the thermal degradation of phase change materials and its nanocomposite used for energy storage applications. Meanwhile Supplementary-Appendix VI: Table T1, provides a comparison between the existing work and uniqueness of current work. The kinetic and thermodynamic parameters will help to determine the relationship between temperature and thermal energy and to understand the accurate prediction of energy requirement to optimize the process at commercial scale.

The current research article is divided into four sections. To begin with Introduction (section 1.0) discusses on the need for the current research with existing research work on the area and the novelty of current research. Subsequently Materials and Methodology (section 2.0) provides complete information regarding the materials used in the experimental research with procurement information, discusses on the procedure adopted in green synthesizing of PJ based nanomaterials and method of its dispersion with organic PCM (PEG) to enhance its thermophysical characteristics as

well elaborates the method involved in determining the kinetic and thermodynamic parameters involved in the thermal degradation of developed nanocomposite PCM via Coats-Redfern method. Furthermore, detailed experimental thermal characteristics results of PEG+CS nanocomposites and the numerically determined kinetic and thermodynamic parameters involved in degradation of nanocomposite samples are presented and discussed along with the inference and insights for the readers are elaborated in Results and Discussion (section 3.0). To conclude with Conclusion (section 4.0) provides the important findings, behaviour of green synthesised nanomaterial with PEG in enhancing there thermophysical characteristics and the outstanding kinetic and thermodynamic parameter determined adopting Coats-Redfern method.

2.0 Materials and Methodology

2.1 Material information

For the current research, we use polyethylene glycol (PEG-1000) acquired from Millipore Sigma as the organic PCM for energy storage. PEG-1000 has a melting temperature ranging between 35-38°C, with latent heat of 146 J/g, density of 1.2 g/cm^3 with white colour appearance. Dried waste weed shrubs of Prosopis Juliflora were acquired from the villages of Tamilnadu in India which is used as the raw material for the green synthesis of PJ nanomaterial.

2.2 Green synthesis of Prosopis Juliflora based Nanoparticle

In this current experimental research investigation of kinetic decomposition analysis, we initial green synthesize PJ nanomaterials using weed shrub of Prosopis Juliflora plant. Figure 1a depicts the synthesis technique adopted in green synthesis of PJ nanoparticle. Initially we collect the dried branks and roots of PJ which is mostly considered as a waste weed plant which drains the ground water level. To proceed with, the dried small pieces of PJ were carbonized under N_2 atmosphere, at a temperature of 1000 °C using tube furnace. Carbonized specks were further processed using hand crushing as a pre-processor to ball mill (Supplementary Appendix-II: Figure S1). To make the particle further smaller we use wet ball milling technique for 3 hours at 300 rpm with a dwell period of 10 minutes between every 20 minutes of operation. The achieved particles were tested using a particle analyzer via dissolving the particle in water to ensure their size in nano scale. Apparently at the end of the synthesis process we achieve PJ based nanomaterial in the size of 300-360 nm and has been used for the research investigation. The elemental composition of green synthesized PJ nanomaterial is provided (Supplementary Appendix-II: Figure S2 & S3), and the proportion of each element is provided in (Supplementary Appendix-II: Table T1).

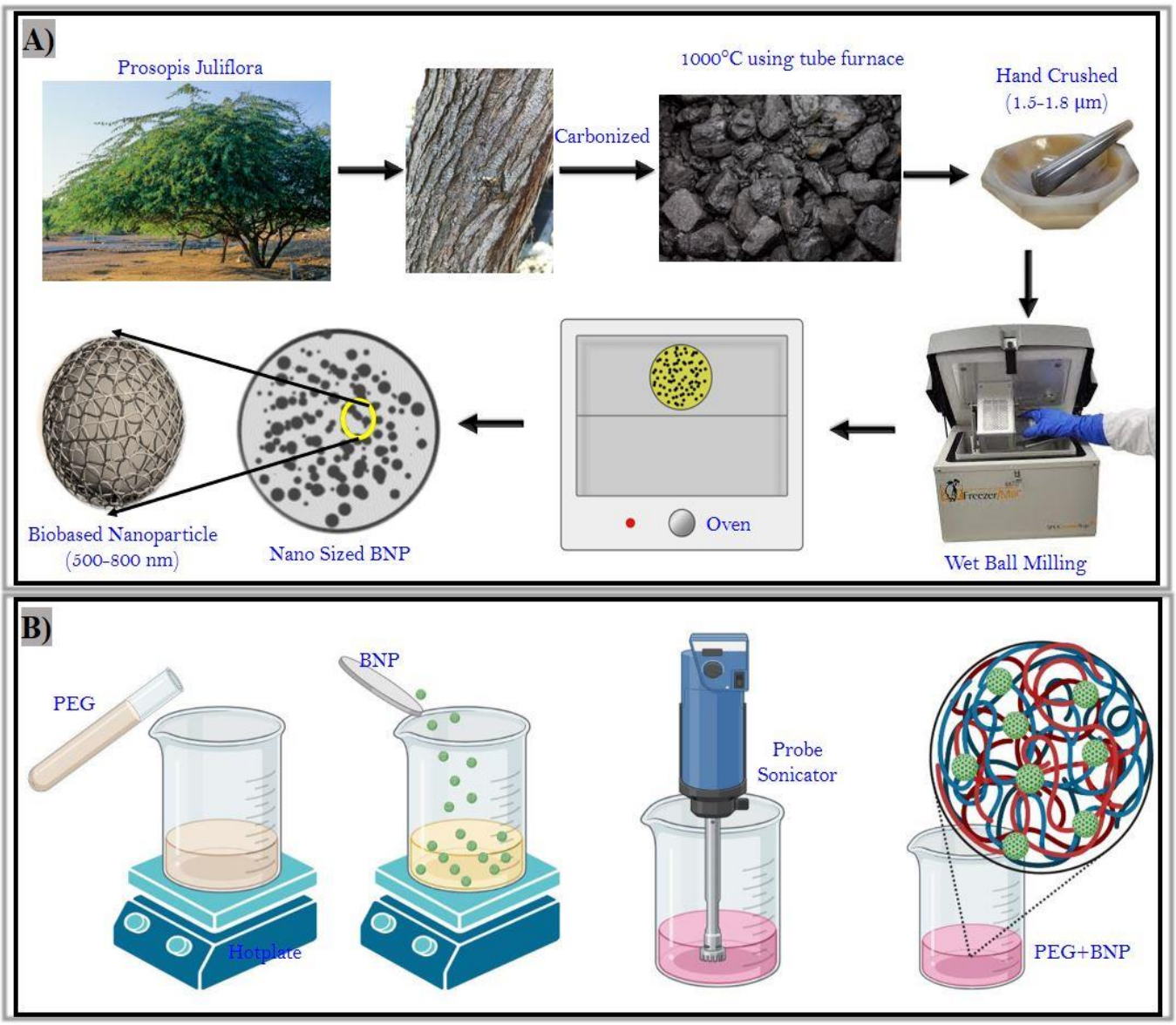

Figure 1: a) Green synthesis process of weed shrub of Prosopis Juliflora into nanomaterial; b) Step by step development process of PJ nanomaterial dispersed organic PCM.

2.3 Development of Prosopis Juliflora Nanoparticle Dispersed Organic PCM

Figure 1b illustrates the preparation and dispersion technique of PJ nanoparticle with organic PCM PEG-1000. We adopt a two-step method to prepare the nanocomposite PCM sample. To begin with, 30 g of PEG-1000 is weighed and melted in a beaker using hot plate maintained at 60°C. Next, we disperse 0.06 g (0.2%) of the synthesised PJ nanomaterial with the liquid state PEG-1000 PCM. The composite mixture is now sonicated using a probe sonicator for 30 minutes and the sample is cooled down to obtain the required green synthesized PJ based nanoparticle dispersed PCM nanocomposite sample, which is considered for further thermal characterization evaluations. Likewise we also developed more samples with weight fraction of 0.4%, 0.6%, 0.8% and 1.0% PJ nanomaterial to determine the optimum level of thermal conductivity.

2.4 Reactivity, Kinetic and Thermodynamics Analysis

2.4.1 Kinetic reaction model and their mechanism

For determining the reaction model during thermal decomposition process one of the most accurate techniques is Coats and Redfern methods. The kinetic factors and the reaction rate involved in the thermal decomposition of Prosopis Juliflora bio nanomaterial dispersed PCM nanocomposite and the pure organic PCM is initiated from Arrhenius law (Akbi et al. 2023), as presented in equation (1), which delivers details in regard to the reaction rates:

$$\frac{d\alpha}{dt} = k(T)f(\alpha) \quad (1)$$

In addition in equation (1), $f(\alpha)$ varies for all the 13 reaction model as itemized in Table1; and $k(T) = A\exp\left(\frac{-E_a}{RT}\right)$; where, A is exponential factor; E_a is activation energy in kJ/mol; R is the gas constant (8.314 J mole^{-1} K^{-1}); T is absolute temperature in (K) and α is a conversion factor (Cebeci, Açıkalın and Figen 2023), the value of conversion factor can be determined using equation (2):

$$\alpha = \frac{(W_i - W_0)}{(W_i - W_f)}, \quad (2)$$

Where initial and final weights of the samples are denoted using W_i and W_f; likewise, weight of the nanocomposite sample at their designated point is represented using W_0. All the weight information is obtained from the TGA analysis result conducted at different heating rates. And equation (3) gives the generic co-relation of Coats and Redfern technique (Waheed, Akogun and Enweremadu 2023):

$$\ln\left(\frac{g(\alpha)}{T^2}\right) = \ln\frac{AR}{\beta E_a}\left(1 - \frac{2RT}{E_a}\right) - \frac{E_a}{RT} \quad (3)$$

Wherein g(α) in equation (3) is an integral function, and varies similar to $f(\alpha)$ as per the reaction models and type of mechanisms as itemized in Table 1; conversely β is the heating rates. The Coats–Redfern technique is a curve-fitting approach that is widely adopted to estimate the pre-exponential factor (A) and activation energy (E_a). We calculate the values of E_a and A by evaluating the slope and intercept of the 1/T vs. ln[g(α)/T²] plot.

Table 1: Kinetic models along with the conversion functions used under Coats-Redfern Method.

Kinetic Reaction Model	Type of Mechanism	Symbol	f(α)	g(α)
Power law	Power law	P2	$2\alpha^{1/2}$	$\alpha^{1/2}$
	Power law	P3	$3\alpha^{1/3}$	$\alpha^{1/3}$
	Power law	P4	$4\alpha^{3/4}$	$\alpha^{1/4}$

Diffusivity model	Parabolic law	D1	$1/(2\alpha)$	α^2
	Valensi equation	D2	$[-ln(1-\alpha)]^{-1}$	$[(1-\alpha)\,ln(1-\alpha)]+\alpha$
	Ginstling-Broushtein equation	D3	$3/2(1-\alpha)^{2/3}[1-(1-\alpha)^{1/3}]^{-1}$	$[1-(1-\alpha)^{1/3}]^2$
Geometrical contraction models	Contracting cylinder	G2	$2(1-\alpha)^{1/2}$	$1-(1-\alpha)^{1/2}$
	Contracting sphere	G3	$3(1-\alpha)^{2/3}$	$1-(1-\alpha)^{1/3}$
Nucleation models	Avarami-Erofe'ev	AE2	$2(1-\alpha)\,[-\ln(1-\alpha)]^{1/2}$	$[-\ln(1-\alpha)]^{1/2}$
	Avarami-Erofe'ev	AE3	$3(1-\alpha)\,[-\ln(1-\alpha)]^{2/3}$	$[-\ln(1-\alpha)]^{1/3}$
	Avarami-Erofe'ev	AE4	$4(1-\alpha)\,[-\ln(1-\alpha)]^{3/4}$	$[-\ln(1-\alpha)]^{1/4}$
Reaction order model	First-order (Mampel)	R1	$(1-\alpha)$	$-ln(1-\alpha)$
	Second-order (Chemical reaction)	R2	$(1-\alpha)^2$	$(1-\alpha)^{-1}-1$

2.4.2 Thermodynamic parameters evaluation

Important thermodynamic parameters like change in enthalpy (ΔH); change in Gibbs free energy (ΔG); and change in entropy (ΔS), can be derived directly using the TGA and kinetic decomposition parameters using the below equations (4, 5 & 6) (Tariq et al. 2023)

$$\Delta H = E_a - RT \quad (4)$$

$$\Delta G = E_a + RT_m \ln\left(\frac{K_B T_m}{hA}\right) \quad (5)$$

$$\Delta S = \Delta H - \Delta G/T_m \quad (6)$$

Where K_B represents the Boltzmann constant (1.381×10^{-23} m^2 kg s^{-2}), h denotes Planck's constant (6.626×10^{-34} m^2 kg s^{-1}), and T_m denotes the peak temperature at which maximum DTG peak lies, it is inferred from TGA plot. As well additional information on material characterization and instrumentation are provided in Supplementary-Appendix I.

3.0 Results and Discussion

The current research is focused on exploring the kinetic and thermodynamic parameters involving degradation mechanism of organic PCM and its nanocomposites. Nonetheless, initially a sustainable nanomaterial is developed using PJ by adopting a green synthesis technique, possessing higher thermal conductive nature to enhance the thermal characteristic of organic energy storage material. In continuation, PJ nanomaterials are blended with organic PCM (PEG-1000) to regulate the optimum weight fraction for better thermal conductivity. PCM and nanocomposite PCM with PJ nanomaterial with higher thermal conductivity is further tested, using TGA at different heating rates to exhibit the degradation chemical mechanism profiles.

3.1 Thermal Conductivity evaluation

In this section we experimentally, determine the optimum weight fraction of PJ nanomaterial to enhance the thermal conductivity of organic PCM (PEG-1000). Henceforth, a biodegradable; economically viable and waste weed plant is opted as the raw material to green synthesize of PJ nanomaterial with higher thermal conductivity than the base PCM. With the help of TEMPOS thermal analyzer, thermal conductivity of base PEG-1000 nanocomposite and PJ nanomaterials dispersed nanocomposites namely PEG+PJ0.2%; PEG+PJ0.4%; PEG+PJ0.6% ; PEG+PJ0.8%; PEG+PJ1.0 is experimentally determined at 20°C. Thermal conductivity improvement on inclusion of the developed nanomaterial with PEG-1000 is illustrated using Figure 2, and we observe a non-linear incremental pattern as the green synthesized PJ nanomaterials are increased from 0.2% to 1.0%. It can be inferred that using the developed nanomaterial the thermal conductivity of PEG-1000 to increases from 0.282 W/m·K to 0.462 W/m·K contributing to about 63.8% increment at a concentration of 0.8wt%. This phenomenon is ascribed owing to the distribution of higher conductivity materials acting as an intermediator within the low conductive PCM matrix. PJ nanomaterial dispersed with the PCM matrix develops thermal network in all horizontal and vertical directions and initiates energy transfer at the tips of PCM. As well owing to the higher surface to volume ratio of PJ nanoparticle conversely lead in improving the mobility of nanomaterials and quickens the phonon interaction (Balasubramanian et al. 2023). In contrast, further inclusion of nanoparticle with PEG-1000 at a concentration of 1.0wt% results in thermal conductivity of 0.431 W/m·K with 52.8% increment owing to clustering and sedimentation effect (Kalidasan et al. 2023b). In addition, high concentration of nanoparticles confines the mean free path for intermolecular collisions which affects the thermal conductivity. Subsequently, based on the thermal conductivity experimental result we preferred to process the nanocomposite PEG+PJ0.8% for further thermal decomposition analysis to compare and contrasts its performance in comparison with the base PCM (PEG-1000).

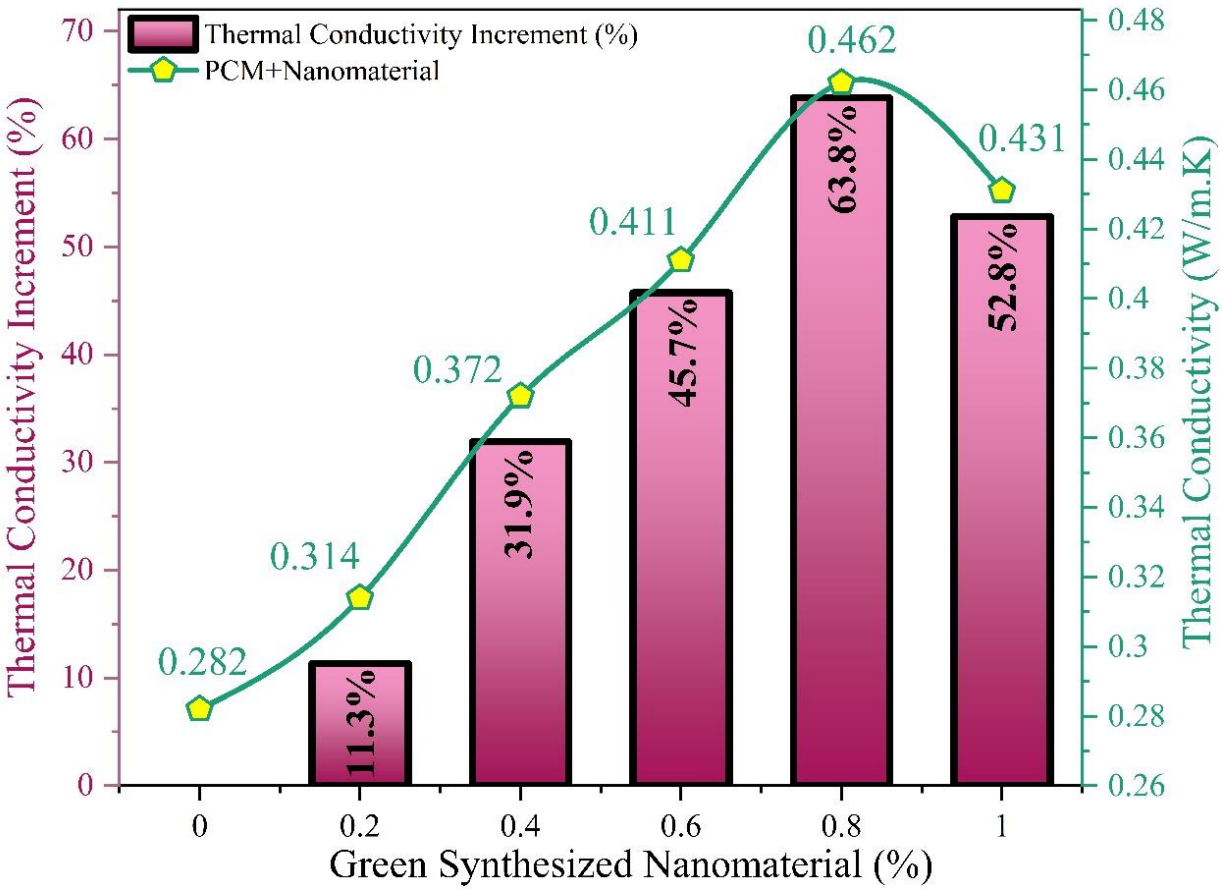

Figure 2: Variation in thermal conductivity of nanocomposite PCM with respect to different weight fraction of green synthesised nanomaterial

3.2 TGA and DTG Analysis

Thermal stability, thermal degradation/decomposition of the developed nanocomposite and the base PCM are evaluated using thermogravimetric analyzer at different heating rates. Figure 3 depicts the thermogravimetric (TG) curves and differential of thermogravimetric (DTG) curves of PCM (PEG-1000) samples at 05°C/min, 10°C/min, 15°C/min and 20°C/min. Likewise Figure 4 depicts the thermogravimetric (TG) curves and differential of thermogravimetric (DTG) curves of PCM+PJ nanomaterial sample at 05°C/min, 10°C/min, 15°C/min and 20°C/min. Results of TGA plots are represented as weight loss of the sample taken with temperature as a variable function. In the current work the samples are decomposed by raising the temperature from 30°C to 500°C based on the aforementioned heating rates. For uniformity, the sample initial size was measured at 4±0.3 mg in an Al_2O_3 crucible pan under N_2 environment (purity of 99.5%). Information regarding stage-by-stage decomposition (weight loss percentage), residue weight, DTG_{max} (°C) can be inferred from plots in Figure 3 & Figure 4 for respective samples at varying heating rates. The decomposition of samples occur in the following stage a) drying stage (30°C-110°C); b) low volatile stage (110°C-220°C); c) pyrolysis stage (220°C-400°C) and d) char stage (400°C-700°C). Heating rates of TGA analysis plays a vital role in identifying the weight loss percentage in drying and volatile stage. Quicker the heating

rates, the probability for absence of peak indicating the loss of volatile matter is higher and the sample spends less time at each temperature point at low heating rates decomposition of sample in all stage are well inferred as can be compared from Figure 3a & 3b (low heating rates; presence of both volatile and pyrolysis decomposition stage) and Figure 3c & 3d (high heating rates, presence of pyrolysis decomposition stage).

When the PCM samples are heated at 5°C/min the decomposition of pure PCM occurs at a slow stride in the drying stage and we observe the minor peak of weight loss, with further increase in heating rates to 10°C/min the peak still exist but with minor variation. Whereas at heating rates of 15°C/min and 20°C/min we observe only decomposition peak of pyrolysis stage, which is attributed due to the higher heat source supplied resulting in very quicker degradation rate and doesn't forms peak to observe the minor change. Lower heating rates provide better resolution of thermal events in a sample. This means that at slower heating rates, you can distinguish between closely spaced decomposition events or reactions that occur over a narrower temperature range. As well it can be inferred from Figure 3a that the residue of PCM is 1.91% at 05°C/min, from Figure 3b the residue is 1.17% at 10°C/min, Figure 3c shows residue to be 1.07% at 15°C/min and finally 0.18% at 20°C/min. As well, it is worth exploring PEG-1000 sample at heating rates of 10°C/min for more discussion, as it's the commonly preferred heating rates in most research as optimum value. TGA curve results shows with rise in temperature of the PCM from 30-500°C, results in thermal degradation profile with three stages of decomposition; stage I (34-202°C) with negligible decomposition, stage II (202-368°C) with initiation for degradation and stage III (368-430°C) maximum and sudden degradation of the samples occurs. This decomposition plots of PEG PCM samples at different heating rates are in accordance to the decomposition plots of D-mannitol (Kottala et al. 2023), Paraffin (Kalidasan et al. 2021), RT50 (Kalidasan et al. 2022a) and other commercialized organic PCMs. As well it can be inferred from Figure 4a that the residue of PCM+PJ sample is 2.48% at 05°C/min, from Figure 4b the residue is 2.01% at 10°C/min, Figure 4c shows residue to be 1.56% at 15°C/min and finally 1.35% at 20°C/min. We observe, the influence of heating rate in decomposition of the sample, as at lower heating the residues are quite higher compared to the residue produced at higher heating rates, however the variation is very minimal. The heating rate can help assess the thermal stability of a material. A material that decomposes at a lower temperature but has a higher rate of weight loss may be less thermally stable than one that decomposes at a higher temperature but with a slower rate of weight loss. An uneven decomposition of sample in terms of weight percentage, which is more specifically owing to the inclusion of PJ nanomaterials. The uneven size of the developed PJ nanomaterial on dispersion with PCM materials, tends to retain at high temperature, whereas the base PEG get decomposed and results in uneven residue. Nonetheless at higher heating rates of 20°C/min,

the residue is only 3.82%. For better interpretation we consider the results of PCM+PJ nanocomposite for 10°C/min as in Figure 4b, and we observe; stage I (31.45-342.6°C) where evaporation of moistures and volatile matters occurs and stage II (342.6-416°C) the maximum degradation occurs and above 416 we obtain residues of nanoparticle as they tend to have a higher decomposition temperature. Maximum decomposition occurs within the temperature range of 360-410°C, and this degradation with change in weight fraction of the sample is effectively used for further analysis of decomposition kinetics reaction mechanism and the change in thermodynamic parameter. Early decomposition of the developed PCM nanocomposite is noticed as much of the PCM fills the voids of nanoparticle and establishes a constant curve above 390°C, this is evident from the weight loss fraction. The loss in weight fraction is minimal for nanocomposite PCM, which is owing to the well penetrated PCM molecules within the voids of PJ nanoparticle.

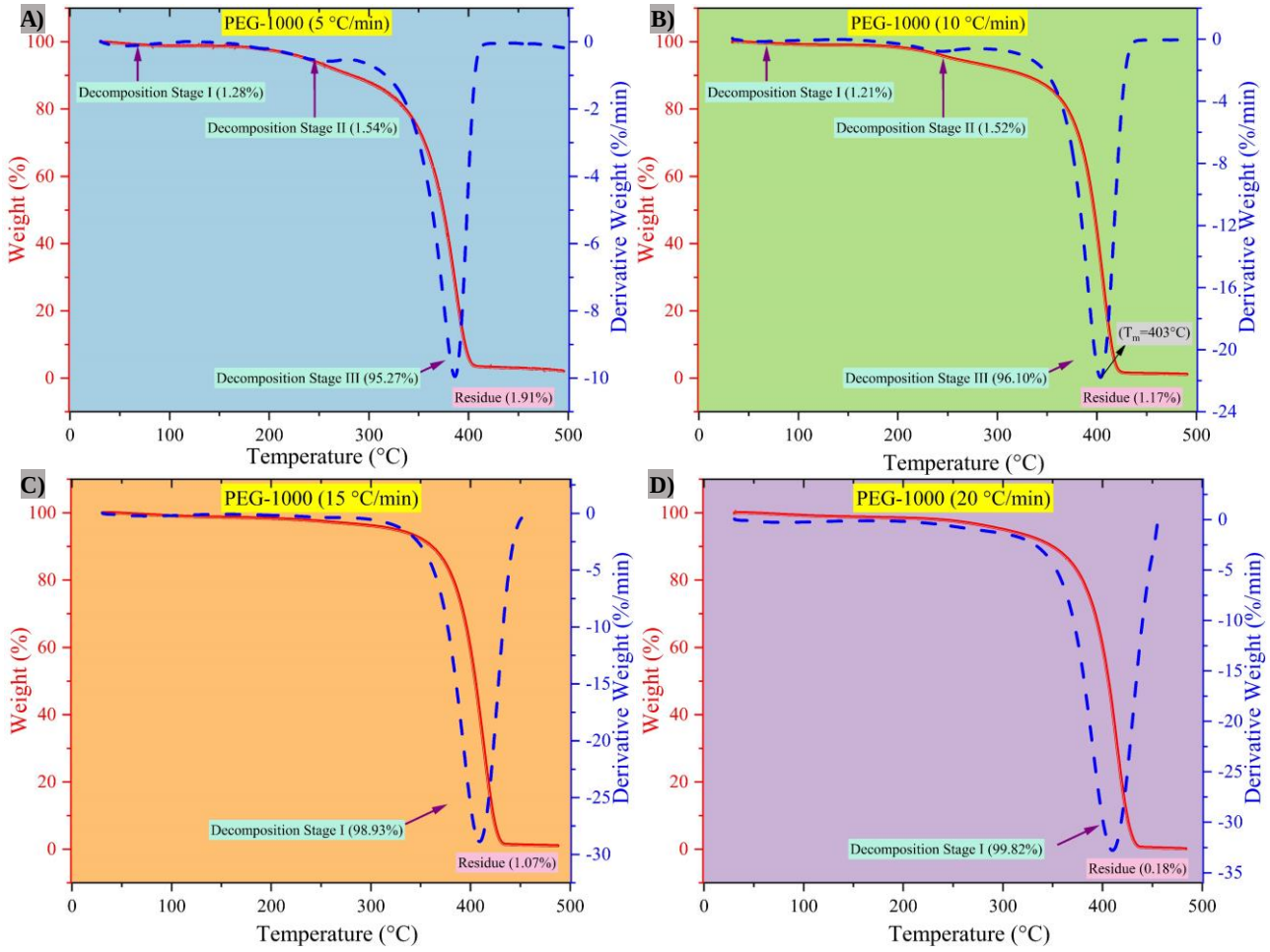

Figure 3: TG and DTG curve of PEG-1000 at heating rates a) 05°C/min; b) 10°C/min; c) 15°C/min and d) 20°C/min

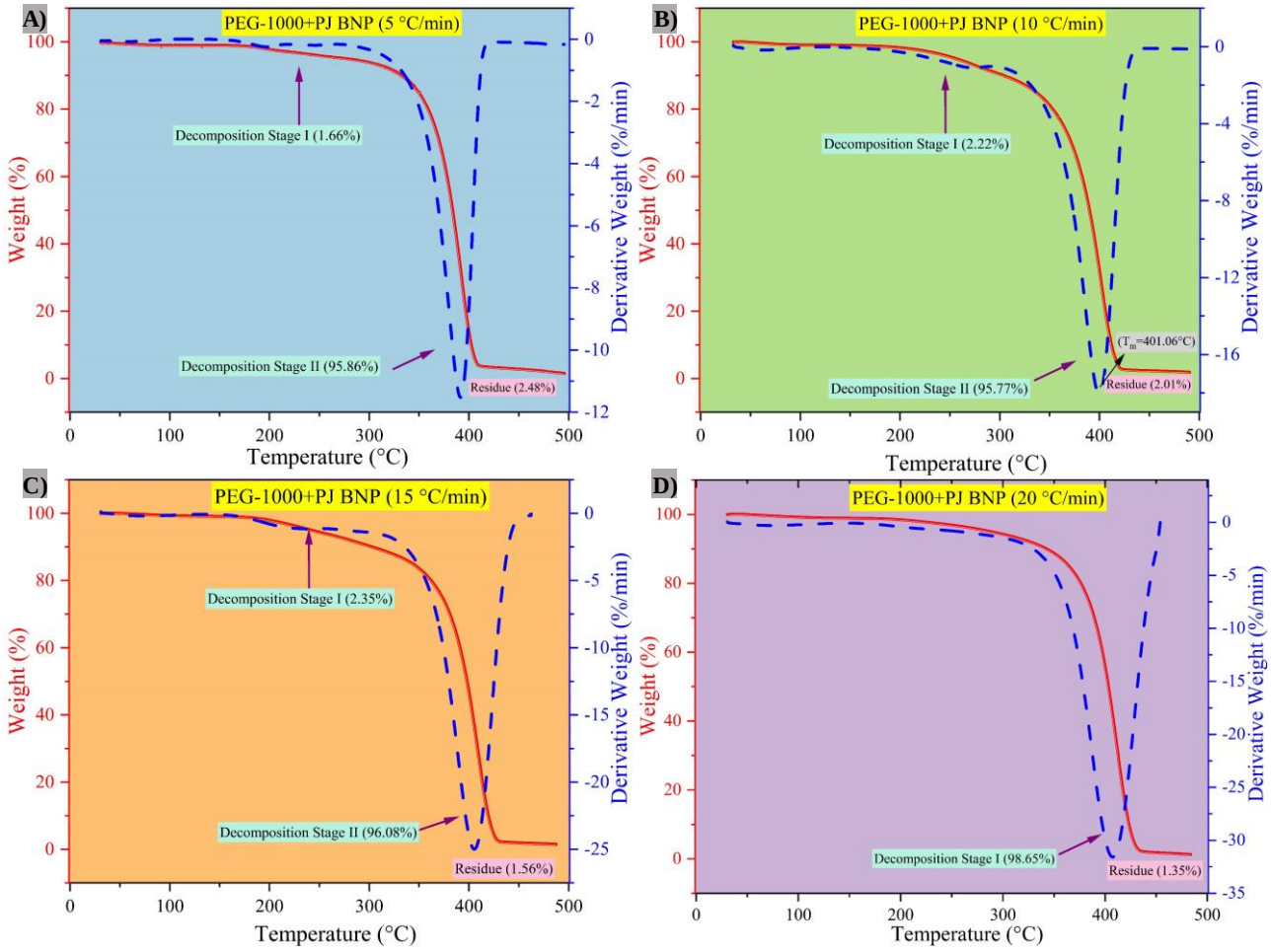

Figure 4: TG and DTG curve of PEG-1000 with 0.8% weight fraction of PJ nanomaterial dispersed PCM at heating rates a) 05°C/min; b) 10°C/min; c) 15°C/min and d) 20°C/min

It is been observed that the weight percentage of PEG and its nanocomposite with PJ nanomaterial predominantly decreases with increase in heating value, where the sample decomposed quicker resulting in higher yield of volatile material (Qiao et al. 2018). In terms of DTG_{max}, the temperature value of PEG-1000 and its nanocomposite shows an increasing trend with increase in heating rates. DTG_{max} for PEG-1000 at 05°C/min, 10°C/min, 15°C/min and 20°C/min are 389.2°C, 401.6°C, 404.3°C and 410.9°C respectively. Conversely DTG_{max} for PJ nanomaterial dispersed nanocomposite PCM at 05°C/min, 10°C/min, 15°C/min and 20°C/min are 398.3°C, 402.4°C, 405.8°C and 413.7°C correspondingly. Higher DTG_{max} of nanocomposite sample compared to the PEG sample, ensures the thermal stability of the sample which is preferred for practical energy storage application. TGA comparison curve of pure PEG-1000 and PJ dispersed PEG-1000 composite samples at different heat rate are presented (Supplementary-Appendix III: Figure S4-S5).

3.3 Kinetic Analysis

In continuation to the illustration of decomposition behaviour of PCM and PJ nanomaterial dispersed PCM nanocomposite, several other kinetic analyses is conducted using the TGA results. Kinetic

parameters were evaluated using the kinetic mechanism functions of Coats–Redfern method as tabulated in Table 1. As an initial process, using numerical data obtained from TGA, we determine g(α) for all the kinetic mechanism followed by extracting a linear regression relationship between $\ln[g(\alpha)/T^2]$ and 1/T for all mechanism at all heating rates to determine m (gradient/slope), c (intercept) and R^2 (fit of curve). Based on R^2 value and linear correlation close significant mechanism can be opted. Mechanism model with regression coefficient in the range of 0.9-0.99 is considered to be more accurate. As maximum decomposition is observed between temperature range of 360-410°C being the active pyrolysis zone, henceforth the linear regression is expressed within that temperature range. Slope obtained using equation (1) gives Ea and intercept value helps in calculating the value of A. Table 2 consolidates the value of Ea, R^2 and A (exponential factor) for all the reaction mechanism for both PCM and PCM+PJ at heating rates of 05°C/min, 10°C/min, 15°C/min & 20°C/min. The regression fit used to determine Ea, and A for heating rate 10°C/min corresponding to each of the mechanism involved in Coats-Redfern technique is provided in Supplementary-Appendix V for PCM and for PJ+PCM nanocomposite.

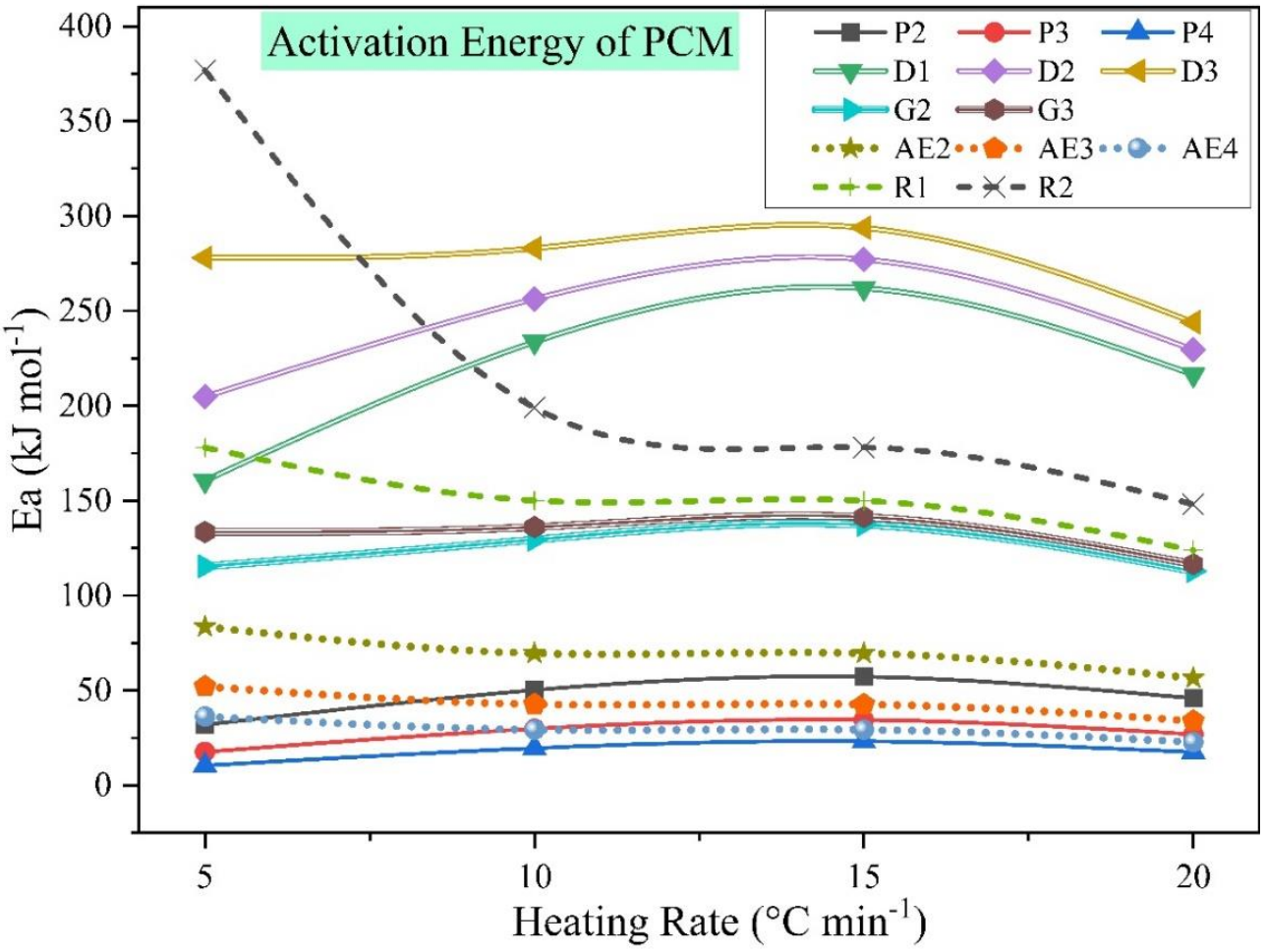

Figure 5: Activation energy for PCM sample under different heating rates for different mechanism of Coats and Redfern model

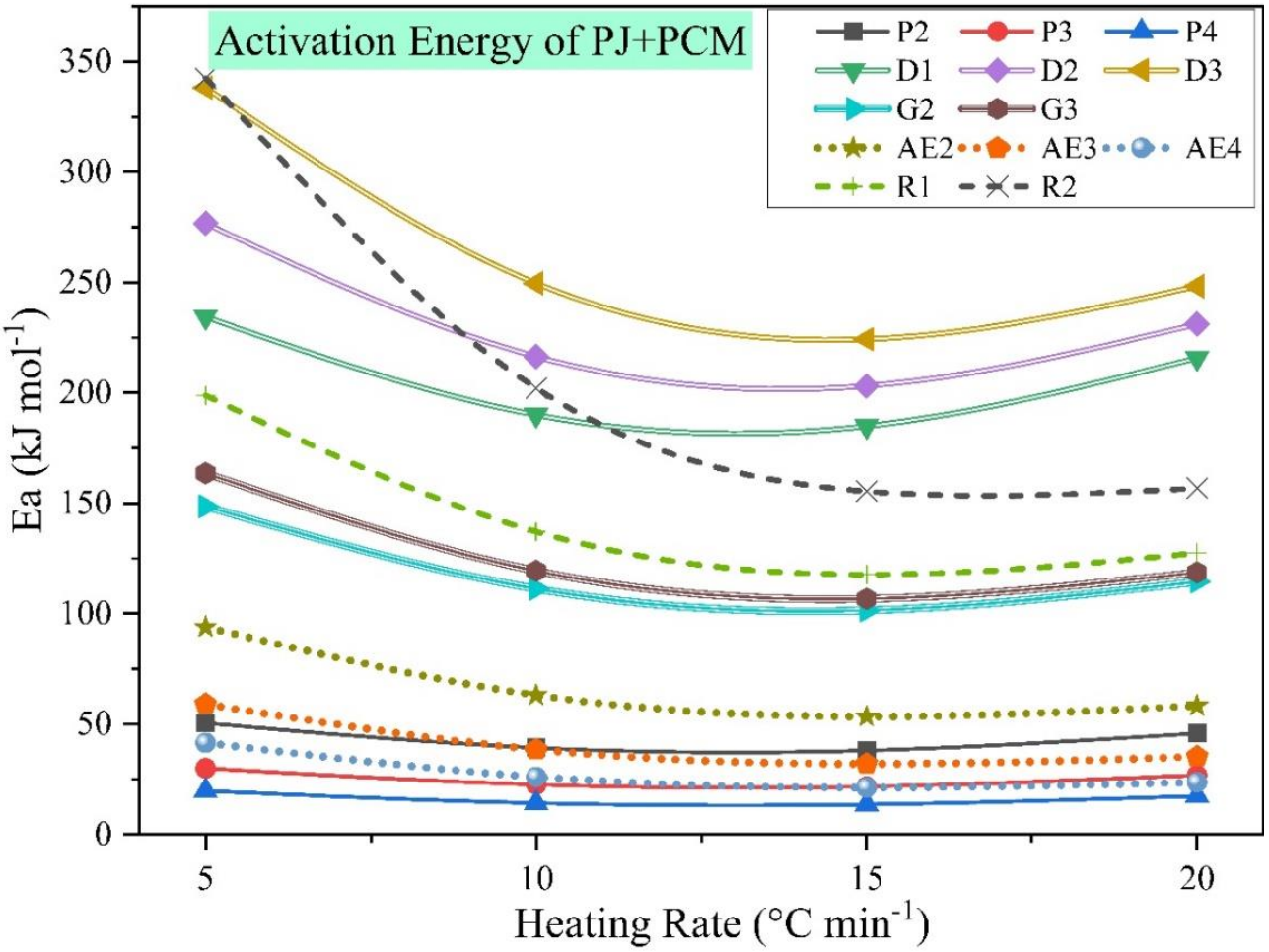

Figure 6: Activation energy for PJ+PCM sample under different heating rates for different mechanism of Coats and Redfern model

Activation energy (Ea) explains the energy barrier that reactant molecules must overcome to initiate a chemical reaction. It quantifies the minimum energy required for reactants to reach a transition state where chemical bonds can break and new bonds can form, facilitating the conversion of reactants into products. As can be inferred in Figure 5, Ea for all chemical model exhibits an increasing trend except the reaction order model, with increase in heating rates until 15°C/min and decreases slightly on further increase in heating rates up to 20°C/min. High Ea is obtained by three dimension diffusion Ginstling-Broushtein equation for all heating levels, which is similar to the activation energy obtained by Tariq et al. (Tariq et al. 2023) for Jute (jeans waste). Conversely, the power law (P2, P3, P4) results in lower value of Ea for the heating values studied. A higher Ea indicates a more significant energy barrier, resulting in slower reaction rates, while a lower Ea signifies a smaller barrier and faster reaction kinetics. The variation in Ea for PJ nanocomposite PCM with respect to all mechanism at different heating rates are illustrated in Figure 6. Inclusion of PJ nanomaterial with PCM has reduced the activation energy required for the reaction to occur considerably. On evaluation we achieve 8-19% decrease in activation energy for the nanocomposite

sample than pure PCM. The reduction in activation energy for PCM with PJ is owing to a) improvement in thermal conductivity, enhances better heat transfer rate and fastens the pyrolysis process resulting in lower value of activation energy; b) PJ nanomaterials exhibit a catalytic effect and c) higher carbon content of PJ improves better decomposition rate on supply of external heat source. Conversely, with increase in heating rates, Ea depicts a decreasing trend up to 15°C/min, and then increases slight at heating rates of 20°C/min. Despite, we notice high activation energy for three dimension diffusion (D3) reaction and lower value of activation for power law (P4). The change in pattern of activation energy, might be owing to the fact that dispersion of PJ nanomaterial with PCM for thermal conductivity increment has undergone carbonization process in controlled atmosphere for developing the weed shrub of PJ into useful nanoparticle. Owing to which all Ea, for PJ nanocomposite PCM are lesser compared to the Ea values of PCM on comparison with corresponding heating value and reaction mechanism. Based on the opted 13 kinetic mechanism reactions, we notice P2, P3, P4 (power law reaction), and nucleation model reaction to exhibit a most possible and quicker reactions to occur in decomposition of the sample. Pekdemir et al. (Pekdemir, Aydoğmuş and Arslanoğlu) also investigated the kinetic analysis of poly(N-isopropylacrylamide) nanocomposite with and without coating of metallic oxide nanoparticles via Coats and Redfern method and response surface methodology and proved that mixing of two nanomaterials can significantly effect the activation energy.

Table 2: Kinetic Reaction Mechanism Parameters of PCM and PCM+PJ nanocomposite during pyrolysis process in temperature range (360-410°C) of via Coats and Redfern Method

Model Name	*Heating Rate (°C/min)*	*PCM (@ temperature 360-410°C)*			*PCM+PJ0.8% (@ temperature 360-410°C)*		
		Ea kJ/mole	*R^2*	*A min^{-1}*	*Ea kJ/mole*	*R^2*	*A min^{-1}*
P2	5	31.954859	0.9452	1.65E+09	50.3795144	0.982	1.02E+08
	10	50.212403	0.9825	1.32E+08	39.2903012	0.994	6.56E+08
	15	57.2859542	0.9899	51022961	38.0298988	0.9811	9.15E+08
	20	45.9065824	0.9832	3.2E+08	45.735314	0.983	3.11E+08
P3	5	17.6581046	0.9213	1.16E+10	29.9403768	0.9772	2.28E+09
	10	29.8298006	0.9784	2.71E+09	22.5492308	0.9921	7.03E+09
	15	34.5455014	0.988	1.53E+09	21.7070226	0.9749	8.69E+09
	20	26.9598078	0.9789	4.75E+09	26.8442432	0.9786	4.65E+09
P4	5	10.5105588	0.9793	2.47E+10	19.720808	0.9703	9.18E+09
	10	19.637668	0.9726	1.05E+10	14.1786956	0.9892	1.91E+10
	15	23.1744436	0.9853	7.25E+09	13.5460002	0.9648	2.21E+10
	20	17.4860048	0.9725	1.55E+10	17.3987078	0.972	1.52E+10

D1	5	160.6182	0.9652	3.07056E+13	234.3301	0.9869	1.90227E+19
	10	233.66497	0.9867	7.39362E+18	189.958272	0.9957	3.64E+15
	15	261.949198	0.9921	6.9952E+20	184.928302	0.9867	9.02E+14
	20	216.430048	0.9876	1.63609E+17	215.756614	0.9874	1.81E+17
D2	5	204.7821	0.9814	9.07044E+16	276.7232	0.9945	3.45417E+22
	10	256.328934	0.981	2.99E+20	216.438362	0.9912	3.25E+17
	15	277.10562	0.9892	6.55E+21	203.127648	0.9818	1.61E+16
	20	229.574482	0.9843	1.06E+18	231.095944	0.9836	1.8E+18
D3	5	277.93702	0.9925	2.86E+22	338.13038	0.9964	9.98E+26
	10	283.075072	0.9728	1.16E+22	249.62785	0.9827	4.57E+19
	15	293.783504	0.9856	3.63E+22	224.22858	0.9752	2.22E+17
	20	243.990958	0.9804	3.92E+18	248.231098	0.9788	1.12E+19
G2	5	115.414948	0.9891	5.84E+09	148.479726	0.9968	2.26E+12
	10	129.473922	0.975	3.68E+10	111.191436	0.9858	1.56E+09
	15	137.297396	0.9865	1.09E+11	101.439114	0.9762	1.85E+08
	20	112.954004	0.9808	1.14E+09	114.408954	0.9794	1.71E+09
G3	5	133.497898	0.9919	1.39E+11	163.594578	0.9962	2.88E+13
	10	136.066924	0.9707	8.99E+10	119.34747	0.9812	5.27E+09
	15	141.42114	0.9846	1.64E+11	106.643678	0.9728	3.49E+08
	20	116.529024	0.9787	1.55E+09	118.649094	0.9769	2.64E+09
AE2	5	83.530758	0.9854	32260550	93.881688	0.9866	1.9E+08
	10	69.58818	0.9555	5025118	63.0982716	0.9655	11751139
	15	69.5266564	0.9775	6427897	53.3575892	0.9588	69149900
	20	56.4952928	0.9697	52713704	58.2703318	0.9666	36803821
AE3	5	52.0431458	0.9834	50917625	58.9445972	0.9851	19219808
	10	42.746431	0.9483	3.37E+08	38.4214882	0.9593	5.86E+08
	15	42.7056924	0.9738	4.03E+08	31.92576	0.9498	1.82E+09
	20	34.0183938	0.9635	1.56E+09	35.2006446	0.9599	1.24E+09
AE4	5	36.298924	0.981	6.43E+08	41.474389	0.9833	3.19E+08
	10	29.3259722	0.9393	2.5E+09	26.0826808	0.9511	3.65E+09
	15	29.2952104	0.9692	2.88E+09	21.2098454	0.9375	8.02E+09
	20	22.78036	0.9551	7.36E+09	23.665801	0.9511	6.28E+09
R1	5	177.994426	0.987	2.48E+15	198.7046	0.9879	7.77E+16
	10	150.117584	0.9612	4.24E+12	137.131116	0.9704	5.32E+11
	15	149.992874	0.9804	2.63E+12	117.651414	0.9655	9.42E+09
	20	123.928484	0.9744	2.02E+10	127.478562	0.9716	4.57E+10
R2	5	376.83205	0.9355	9.34E+31	342.545114	0.9307	7.09E+28
	10	199.062102	0.9281	5.78E+16	202.121654	0.931	1.72E+17
	15	178.119136	0.9656	6.38E+14	155.43023	0.9416	1.64E+13
	20	148.147166	0.9602	2.41E+12	156.84361	0.9539	1.48E+13

In continuation alike activation energy, another significant kinetic factor presenting significant information and insights is the Pre-exponential factor which is denoted as (A). Pre-

exponential factor (A) in Arrhenius equation signifies the occurrence of collision between the PCM and PJ+PCM nanocomposite when decomposed in controlled ambient. Value of pre-exponential factors varies with respect to variation in heating rates. Variation in pre-exponential factor with heating rate of (05°C/min, 10°C/min, 15°C/min and 20°C/min) and different degradation mechanism can be well interpreted from Supplementary-Appendix IV: Figure S6-S9. As pre-exponential factor, is allied to the time taken for the molecules of reactant to collide at different angles, lower value of A ($\leq 10^9$ s^{-1}) specifies that extra surface reactions ensued due to restrictions in the spin of the particles in the activated complex reagent on comparison with the initial substance. Nonetheless, higher values of A ($> 10^9$ s^{-1}) specifies that the sample is packed of loosely bound complex molecules (Akyürek 2019). Irrespective of the type of mechanism (as per Coats-Redfern technique), value of A initially decreases and increases with increase in heating rates from 05°C/min-20°C/min, where we observe a non-linear sinusoidal type of variation on close observation. In almost all heating rates dimensional-diffusion law exhibit higher values of A; signifying maximum collision interaction and correspondingly it can be justified with higher activation energy. Conversely Avrami-Erofeev (AE2, AE3 & AE4) and Power law (P2,P3 & P4) reaction model depicts lowest value of A; for all heating rates in both PCM and its nanocomposite with PJ+PCM, which is in accordance to their lower value of Ea.

3.4 Thermodynamic Analysis

Significant thermodynamic parameters like ΔH, ΔG & ΔS for PCM and PJ+PCM nanocomposite while treating under pyrolysis condition at temperature range of 360-410°C are discussed in this section. Table 3 consolidates the thermodynamic parameter assessed different heating rates from 05°C/min to 20°C/min for all categories of reaction models under Coats-Redfern technique for the PCM sample and its nanocomposites with PJ nanomaterial. In addition, Figure 7 provides a better visualization of the variation in enthalpy ΔH and ΔG with variation in heating rates to exhibit the amount of energy absorbed and energy generated within each reaction. In addition, the entropy change is also portrayed to understand the synergistic effect of the reaction occurring. Change in enthalpy exhibits details on the amount of heat energy absorbed and released by the sample during decomposition reaction (Yuan et al. 2017). It can be inferred from Figure 7a & 7b that for both PCM and PCM+PJ, ΔH is observed to be positive for all reaction mechanisms irrespective of the heating rates, signifying that for the reaction to occur and decompose the molecules into by-product there is a need for external heat input source. Higher the value of ΔH, higher is the reaction duration in converting the sample reactants into by-products, which is expected to make considerable change in the reaction activity. It is also observed that ΔH, adopts a similar configuration as that of Ea with increase in heating rates. Next thermodynamic factor we infer and discuss in the change in Gibbs free

energy. ΔG, represents the amount of energy released during formation of any intermediate compound being the product of bond breakage of the reactant samples. Higher the value of ΔG, lower is the probability of the reaction to occur, in common it supports in determining the change in heat flow and disorderness occurrence. Figure 7c and 7d illustrates a higher value of ΔG for dimension diffusivity model (D1, D2 & D3) and for reaction order model (R1, R2) as compared to nucleation (AE2, AE3 & AE4), geometrical (G2 & G3) and power model (P2, P3 & P4). Unlike ΔH, it is observed that ΔG trace a different path being more inversely proportionate to Ea with increase in heating rates. Predominant change in G is observed with nucleation model and power model on increasing the heating rates, whereas diffusion model, geometric model and reaction model exhibit very minimal variation. Conversely, we obtain a positive value of ΔG for all reaction indicating the reaction to be more non-spontaneous and the need for external energy source for the reaction to happen, which is in accordance with existing research work with other biomass source like jute, rice husk and medical solid wastes.

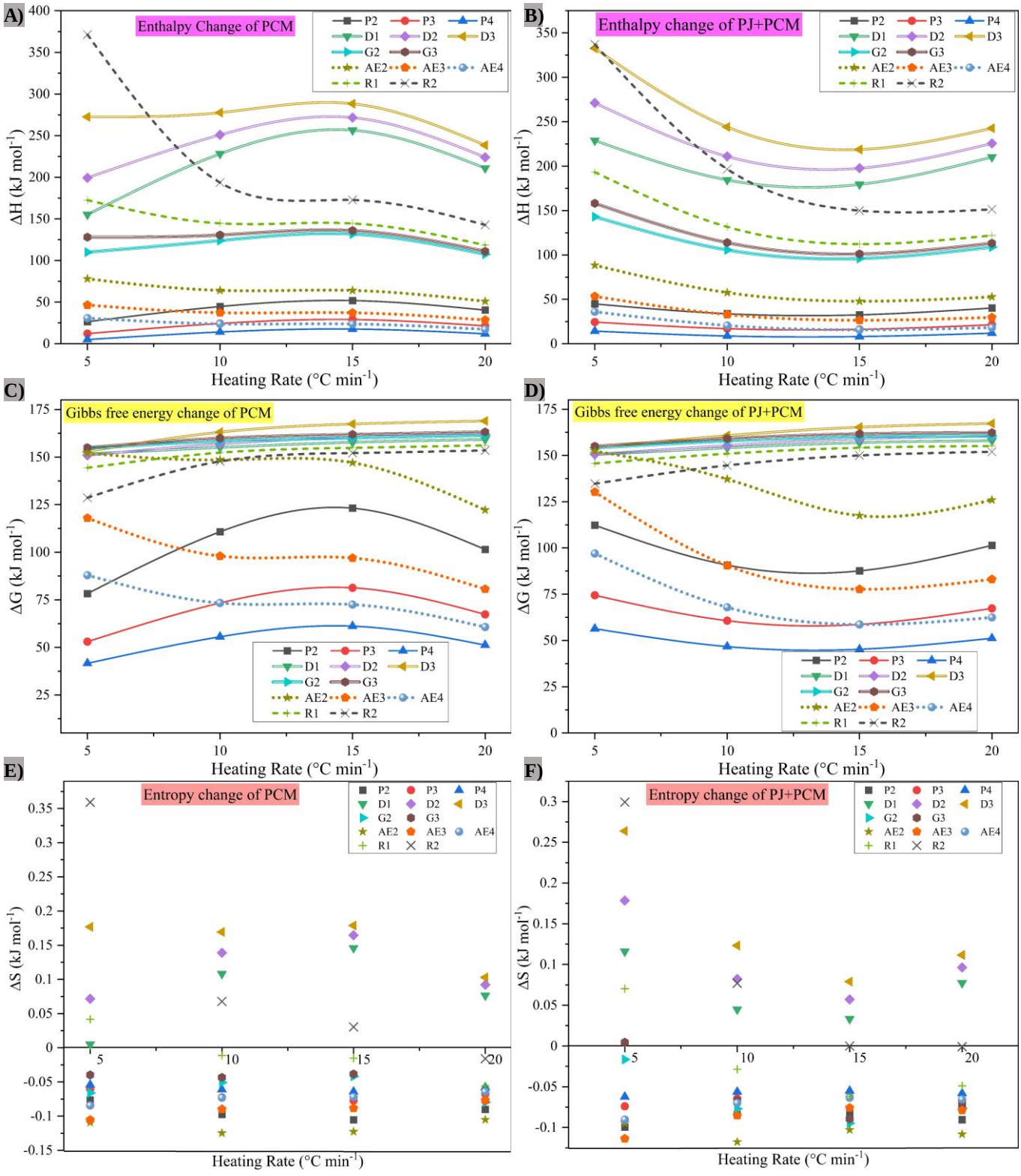

Figure 7: Thermodynamic parameter plots a) Change in enthalpy of PCM; b) Change in enthalpy of PJ+PCM; c) Change in Gibbs free energy of PCM; d) Change in Gibbs free energy of PJ+PCM; e) Change in entropy of PCM and f) Change in entropy of PJ+PCM at different heating rates.

Table 3: Thermodynamic Parameters values of PCM and PCM+PJ nanocomposite during pyrolysis process in temperature range (360-410°C) of via Coats and Redfern Method

Model Name	*Heating Rate (°C/min)*	*PCM (@ temperature 360-410°C)*			*PCM+PJ0.8% (@ temperature 360-410°C)*		
		ΔH *kJ/mole*	ΔG *kJ/mole*	ΔS *kJ/mole*	ΔH *kJ/mole*	ΔG *kJ/mole*	ΔS *kJ/mole*
P2	5	26.483	78.26385	-0.07658	44.90766	112.3207	-0.0997
	10	44.74054	110.7271	-0.09759	33.81844	90.78893	-0.08426
	15	51.8141	123.1448	-0.1055	32.55804	87.66188	-0.0815
	20	40.43472	101.4437	-0.09023	40.26345	101.4349	-0.09047
P3	5	12.18625	52.99739	-0.06036	24.46852	74.4498	-0.07392
	10	24.35794	73.3605	-0.07247	17.07737	60.71696	-0.06454
	15	29.07364	81.2923	-0.07723	16.23516	58.68671	-0.06278
	20	21.48795	67.33454	-0.06781	21.37238	67.33643	-0.06798
P4	5	5.0387	41.6114	-0.05409	14.24895	56.39021	-0.06233
	10	14.16581	55.55606	-0.06121	8.706837	46.72882	-0.05623
	15	17.70258	61.16868	-0.06428	8.074141	45.27615	-0.05502
	20	12.01415	51.21444	-0.05798	11.92685	51.22274	-0.05812
D1	5	155.1463	151.6678	0.005145	228.8582	150.4073	0.116026
	10	228.1931	155.0546	0.108169	184.4864	154.1562	0.044857
	15	256.4773	157.7622	0.145996	179.4564	156.9757	0.033248
	20	210.9582	159.2427	0.076485	210.2848	158.0134	0.077307
D2	5	199.3103	150.9107	0.071581	271.2513	150.615	0.178417
	10	250.8571	156.9158	0.138936	210.9665	155.3929	0.082191
	15	271.6338	160.3475	0.164588	197.6558	158.9689	0.057216
	20	224.1026	161.8639	0.092049	225.6241	160.425	0.096427
D3	5	272.4652	152.8892	0.176848	332.6585	154.2813	0.263813
	10	277.6032	163.097	0.16935	244.156	160.7746	0.123318
	15	288.3116	167.3989	0.178825	218.7567	165.3312	0.079014
	20	238.5191	168.9504	0.102889	242.7592	167.2923	0.111613
G2	5	109.9431	154.6276	-0.06609	143.0079	154.1879	-0.01653
	10	124.0021	158.3345	-0.05078	105.7196	157.8143	-0.07705
	15	131.8255	160.0554	-0.04175	95.96725	160.0631	-0.0948
	20	107.4821	161.3394	-0.07965	108.9371	160.5307	-0.0763
G3	5	128.026	154.909	-0.03976	158.1227	155.0132	0.004599
	10	130.5951	159.9105	-0.04336	113.8756	159.1333	-0.06693
	15	135.9493	161.8991	-0.03838	101.1718	161.6875	-0.0895
	20	111.0572	163.1956	-0.07711	113.1772	162.3147	-0.07267
AE2	5	78.0589	151.9667	-0.10931	88.40983	152.346	-0.09456
	10	64.11632	148.4768	-0.12477	57.62641	137.2114	-0.1177
	15	64.0548	147.0312	-0.12272	47.88573	117.5075	-0.10297
	20	51.02343	122.1709	-0.10522	52.79847	125.9656	-0.10821
AE3	5	46.57129	117.9137	-0.10551	53.47274	130.292	-0.11361
	10	37.27457	97.9994	-0.08981	32.94963	90.56037	-0.0852

	15	37.23383	96.9457	-0.08831	26.4539	77.70287	-0.0758
	20	28.54653	80.64526	-0.07705	29.72879	83.10794	-0.07895
AE4	5	30.82706	87.91793	-0.08444	36.00253	97.02303	-0.09025
	10	23.85411	73.30202	-0.07313	20.61082	67.93127	-0.06999
	15	23.82335	72.48792	-0.07197	15.73799	58.64187	-0.06345
	20	17.3085	60.69218	-0.06416	18.19394	62.46728	-0.06548
R1	5	172.5226	144.3559	0.041657	193.2327	145.7053	0.070291
	10	144.6457	152.3022	-0.01132	131.6593	150.9831	-0.02858
	15	144.521	154.8495	-0.01528	112.1796	154.1781	-0.06211
	20	118.4566	156.1594	-0.05576	122.0067	155.1249	-0.04898
R2	5	371.3602	128.6371	0.358978	337.0733	134.7317	0.299255
	10	193.5902	147.7232	0.067836	196.6498	144.637	0.076925
	15	172.6473	152.1144	0.030367	149.9584	150.0073	-7.2E-05
	20	142.6753	153.4994	-0.01601	151.3718	151.9926	-0.00092

Finally, ΔS signifies the material disorderness (Khan et al. 2016). The concept of entropy change is fundamental in thermodynamics and helps explain the spontaneity and direction of various processes, with nature generally favouring an increase in entropy for spontaneous processes. An increase in entropy ($\Delta S>0$) indicates that the system is becoming more disordered, while a decrease in entropy ($\Delta S<0$) suggests a decrease in disorderness. In can be inferred from Figure 7e & 7f that we do observe both negative and positive values of entropy change. In general, ΔS in (-)ve signifies need for usage of very less amount of energy as the reaction is less disordered. In the current research we observe negative value of ΔS for all samples estimated following nucleation, geometrical and power model irrespective of the heating rates; whereas diffusion and reaction model establishes positive value of ΔS owing to higher change in Gibbs free energy. Furthermore, negative value of ΔS signifies lower randomness in the by-product obtained compared to the initial PCM and PCM+PJ samples. This varied values of ΔS indicates that for thermodynamic equilibrium to attain there is a need for physical and chemical modifications. As well for extended interpretation the internal reaction mechanism of PCM and PCM+PJ nanocomposite samples need to be investigated in future studies to express a comparative analysis.

4.0 Conclusion

In the current research work the authors have developed an eco-friendly green synthesized PJ nanomaterial, and dispersed it with PCM to enhance their thermal property. In addition, the research focuses on the decomposition mechanism of the developed nanocomposite through reactivity, kinetic and thermodynamic parameter adopting the chemical mechanism models of Coats and Redfern method. Nanomaterials developed using branches and root thorny shrub Prosopis Juliflora is noted to establish a significant role in enhancing the thermal conductivity of PEG-1000 by 63.8% with just

0.8 weight fraction. The influence of different heating rates with weight loss fraction and the thermo-kinetic profiles were assessed. The TGA and DTG results showed that the pyrolysis of green synthesised nanomaterial based organic phase change material is a complex process involving a multiple reactions. Thermo-kinetic calculations were executed via the Coats–Redfern method in the active pyrolytic zone (360–410°C). Average maximum activation energy for PCM and PCM+PJ sample in consolidation with all heating rates is observed at three dimensional diffusion reaction mechanism and is 275.46 kJ/mol and 272.55 kJ/mol respectively. However, the range of activation energy varied between 10.5 to 376.8 kJ/mol for PCM samples and 14.1-342.5 kJ/mol for PCM+PJ samples. All thermodynamic parameter ΔH, ΔG & ΔS assessed provide significant inference on the reaction breakdown, mechanism, energy involved, rate of reaction and their disorderness. The dimensional-diffusion law shows greater values of pre exponential factor (A) at practically all heating rates, indicating the highest collision interaction, which can be explained by having a higher activation energy. Subsequently, the need for activation energy for the green synthesised nanomaterial blend phase change material is less compared to the base organic phase change material, which reflects need for low energy for the decomposition breakdown to occur. For most of the reaction mechanisms, in comparison to lower heating rates, higher heating rates offered an enhanced correlation coefficient R^2. The kinetic and thermodynamic parameters enabled us to understand the reaction mechanism, conversion rate, and energy profile. This work will provide a new insight in regard to the disposal of used PCM in a more ecofriendly way adopting pyrolysis technique. Future research works will focus on inorganic and eutectic PCMs and its nanocomposite to explore more about the pyrolysis kinetics of energy storage materials. To make it more feasible, further sustainability investigation and cost-benefit analysis are needed. Another advantageous step to improve reactivity and lower the energy demand at commercial sizes is the use of a suitable catalyst.

References

Açıkalın, K. (2022) Evaluation of orange and potato peels as an energy source: a comprehensive study on their pyrolysis characteristics and kinetics. *Biomass Conversion and Biorefinery,* 12**,** 501-514.

Akbi, H., S. Rafai, A. Mekki, S. Touidjine & K. Belkadi (2023) Kinetic investigation of the multi-step thermal decomposition of graphene oxide paper. *Journal of Thermal Analysis and Calorimetry***,** 1-17.

Akyürek, Z. (2019) Sustainable valorization of animal manure and recycled polyester: co-pyrolysis synergy. *Sustainability,* 11**,** 2280.

Al-Rumaihi, A., P. Parthasarathy, A. Fernandez, T. Al-Ansari, H. R. Mackey, R. Rodriguez, G. Mazza & G. McKay (2021) Thermal degradation characteristics and kinetic study of camel manure pyrolysis. *Journal of Environmental Chemical Engineering,* 9**,** 106071.

Annex, I. Technical guidelines for the environmentally sound management of persistent organic pollutant wastes developed under the Basel Convention on the Control of Transboundary Movements of Hazardous Wastes and their Disposal.

Atinafu, D. G., S. Wi, B. Y. Yun & S. Kim (2021) Engineering biochar with multiwalled carbon nanotube for efficient phase change material encapsulation and thermal energy storage. *Energy,* 216**,** 119294.

Balal, A. T., Y. P. T. Jafarabadi, A. T. Demir, M. T. Igene, M. T. Giesselmann & S. T. Bayne (2023) Forecasting Solar Power Generation Utilizing Machine Learning Models in Lubbock.

Balasubramanian, K., A. K. Pandey, R. Abolhassani, H.-G. Rubahn, S. Rahman & Y. K. Mishra (2023) Tetrapods based engineering of organic phase change material for thermal energy storage. *Chemical Engineering Journal,* 462**,** 141984.

Balasubramanian, R., A. Abishek, S. Gobinath & K. Jaivignesh (2022) Alternative fuel: hydrogen and its thermodynamic behaviour. *J Hum Earth Future. https://doi. org/10.28991/HEF-2022-03-02-05*.

Boopalan, N., B. Kalidasan, K. Ranjith, B. Dhanush, S. Anbarasu & S. P. Selvam. 2021. Experimental study and performance analysis of phase change material integrated stepped slope solar still. In *IOP Conference Series: Materials Science and Engineering*, 012002. IOP Publishing.

Bordoloi, U., D. Das, D. Kashyap, D. Patwa, P. Bora, H. H. Muigai & P. Kalita (2022) Synthesis and comparative analysis of biochar based form-stable phase change materials for thermal management of buildings. *Journal of Energy Storage,* 55**,** 105801.

Cebeci, H. H., K. Açıkalın & A. K. Figen (2023) Recycling of printed circuit board e-wastes: a combined study of pyrolysis characteristics, kinetics and evolved gas analyses at various particle sizes. *Journal of Material Cycles and Waste Management***,** 1-17.

Chen, W., B. Zhang, S. Wang, B. Xue, S. Liu, M. An, Z. Yang & G. Xu (2023) Effect of GO on the Structure and Properties of PEG/Biochar Phase Change Composites. *Polymers,* 15**,** 963.

Das, D., U. Bordoloi, H. H. Muigai & P. Kalita (2020) A novel form stable PCM based bio composite material for solar thermal energy storage applications. *Journal of Energy Storage,* 30**,** 101403.

de Jesus, M. S., A. d. C. O. Carneiro, C. L. M. Martinez, B. R. Vital, A. P. S. Carneiro & M. R. de Assis (2019) Thermal decomposition fundamentals in large-diameter wooden logs during slow pyrolysis. *Wood science and technology,* 53**,** 1353-1372.

El-Sayed, S. A., T. M. Khass & M. E. Mostafa (2023) Thermal degradation behaviour and chemical kinetic characteristics of biomass pyrolysis using TG/DTG/DTA techniques. *Biomass Conversion and Biorefinery***,** 1-25.

Goud, M. & F. Raval (2022) A sustainable biochar-based shape stable composite phase change material for thermal management of a lithium-ion battery system and hybrid neural network modeling for heat flow prediction. *Journal of Energy Storage,* 56**,** 106163.

Hagemann, N., K. Spokas, H.-P. Schmidt, R. Kägi, M. A. Böhler & T. D. Bucheli (2018) Activated carbon, biochar and charcoal: linkages and synergies across pyrogenic carbon's ABC s. *Water,* 10**,** 182.

Hekimoğlu, G., A. Sarı, T. Kar, S. Keleş, K. Kaygusuz, V. Tyagi, R. Sharma, A. Al-Ahmed, F. A. Al-Sulaiman & T. A. Saleh (2021) Walnut shell derived bio-carbon/methyl palmitate as novel composite phase change material with enhanced thermal energy storage properties. *Journal of Energy Storage,* 35**,** 102288.

Kalidasan, B., A. Pandey, S. Rahman, A. Yadav, M. Samykano & V. Tyagi (2022a) Graphene–Silver Hybrid Nanoparticle based Organic Phase Change Materials for Enhanced Thermal Energy Storage. *Sustainability,* 14**,** 13240.

Kalidasan, B., A. Pandey, R. Saidur, R. Kothari, K. Sharma & V. Tyagi (2023a) Eco-friendly coconut shell biochar based nano-inclusion for sustainable energy storage of binary eutectic salt hydrate phase change materials. *Solar Energy Materials and Solar Cells,* 262**,** 112534.

Kalidasan, B., A. Pandey, R. Saidur, M. Samykano & V. Tyagi (2022b) Nano additive enhanced salt hydrate phase change materials for thermal energy storage. *International Materials Reviews***,** 1-44.

Kalidasan, B., A. Pandey, R. Saidur & V. Tyagi (2023b) Energizing organic phase change materials using silver nanoparticles for thermal energy storage. *Journal of Energy Storage,* 58**,** 106361.

Kalidasan, B., A. Pandey, S. Shahabuddin, M. George, K. Sharma, M. Samykano, V. Tyagi & R. Saidur (2021) Synthesis and characterization of conducting Polyaniline@ cobalt-Paraffin wax nanocomposite as nano-phase change material: Enhanced thermophysical properties. *Renewable Energy,* 173**,** 1057-1069.

Karaeva, J. V., S. S. Timofeeva, S. I. Islamova & A. V. Gerasimov (2022) Pyrolysis kinetics of new bioenergy feedstock from anaerobic digestate of agro-waste by thermogravimetric analysis. *Journal of Environmental Chemical Engineering,* 10**,** 107850.

Keeran, N. S., U. Balasundaram, G. Govindan & A. K. Parida. 2019. Prosopis juliflora: a potential plant for mining of genes for genetic engineering to enhance phytoremediation of metals. In *Transgenic plant technology for remediation of toxic metals and metalloids*, 381-393. Elsevier.

Khan, A. S., Z. Man, M. A. Bustam, C. F. Kait, Z. Ullah, A. Nasrullah, M. I. Khan, G. Gonfa, P. Ahmad & N. Muhammad (2016) Kinetics and thermodynamic parameters of ionic liquid pretreated rubber wood biomass. *Journal of Molecular Liquids,* 223**,** 754-762.

Kottala, R. K., B. K. Chigilipalli, S. Mukuloth, R. Shanmugam, V. C. Kantumuchu, S. B. Ainapurapu & M. Cheepu (2023) Thermal Degradation Studies and Machine Learning Modelling of Nano-Enhanced Sugar Alcohol-Based Phase Change Materials for Medium Temperature Applications. *Energies,* 16**,** 2187.

Lv, L., J. Wang, M. Ji, Y. Zhang, S. Huang, K. Cen & H. Zhou (2022) Effect of structural characteristics and surface functional groups of biochar on thermal properties of different organic phase change materials: Dominant encapsulation mechanisms. *Renewable Energy,* 195**,** 1238-1252.

Magnacca, G., F. Guerretta, A. Vizintin, P. Benzi, M. C. Valsania & R. Nisticò (2018) Preparation, characterization and environmental/electrochemical energy storage testing of low-cost biochar from natural chitin obtained via pyrolysis at mild conditions. *Applied Surface Science,* 427**,** 883-893.

Mandal, S., S. Ishak, D.-E. Lee & T. Park (2022) Optimization of eco-friendly Pinus resinosa biochar-dodecanoic acid phase change composite for the cleaner environment. *Journal of Energy Storage,* 55**,** 105414.

Ming, X., F. Xu, Y. Jiang, P. Zong, B. Wang, J. Li, Y. Qiao & Y. Tian (2020) Thermal degradation of food waste by TG-FTIR and Py-GC/MS: pyrolysis behaviors, products, kinetic and thermodynamic analysis. *Journal of Cleaner Production,* 244**,** 118713.

Naveenkumar, R., M. Ravichandran, V. Mohanavel, A. Karthick, L. S. R. L. Aswin, S. S. H. Priyanka, S. K. Kumar & S. P. Kumar (2022) Review on phase change materials for solar energy storage applications. *Environmental Science and Pollution Research,* 29**,** 9491-9532.

Nawaz, A. & P. Kumar (2022) Thermal degradation of hazardous 3-layered COVID-19 face mask through pyrolysis: Kinetic, thermodynamic, prediction modelling using ANN and volatile product characterization. *Journal of the Taiwan Institute of Chemical Engineers,* 139**,** 104538.

Oyewola, O. M., A. A. Awonusi & O. S. Ismail (2022) Performance improvement of air-cooled battery thermal management system using sink of different pin-fin shapes. *Emerging Science Journal,* 6**,** 851-865.

Pekdemir, E., E. Aydoğmuş & H. Arslanoğlu Thermal decomposition kinetics of synthesized poly(N-isopropylacrylamide) and Fe3O4 coated nanocomposite: Evaluation of calculated activation energy by RSM. *Petroleum Science and Technology***,** 1-18.

Qiao, Y., F. Xu, S. Xu, D. Yang, B. Wang, X. Ming, J. Hao & Y. Tian (2018) Pyrolysis characteristics and kinetics of typical municipal solid waste components and their mixture: analytical TG-FTIR study. *Energy & fuels,* 32**,** 10801-10812.

Sheng, N., Z. Rao, C. Zhu & H. Habazaki (2020) Honeycomb carbon fibers strengthened composite phase change materials for superior thermal energy storage. *Applied Thermal Engineering,* 164**,** 114493.

Subramanian, M., A. T. Hoang, B. Kalidasan, S. Nižetić, J. M. Solomon, D. Balasubramanian, C. Subramaniyan, G. Thenmozhi, H. Metghalchi & X. P. Nguyen (2021) A technical review on composite phase change material based secondary assisted battery thermal management system for electric vehicles. *Journal of Cleaner Production,* 322**,** 129079.

Tariq, R., A. Inayat, M. Shahbaz, H. Zeb, C. Ghenai, T. Al-Ansari & J. Kim (2023) Kinetic and thermodynamic evaluation of pyrolysis of jeans waste via coats-redfern method. *Korean Journal of Chemical Engineering,* 40**,** 155-161.

Tyagi, V., K. Chopra, B. Kalidasan, A. Chauhan, U. Stritih, S. Anand, A. Pandey, A. Sarı & R. Kothari (2021) Phase change material based advance solar thermal energy storage systems for building heating and cooling applications: A prospective research approach. *Sustainable Energy Technologies and Assessments,* 47**,** 101318.

Waheed, M., O. Akogun & C. Enweremadu (2023) Influence of feedstock mixtures on the fuel characteristics of blended cornhusk, cassava peels, and sawdust briquettes. *Biomass Conversion and Biorefinery***,** 1-16.

Xiong, T., Y. S. Ok, P. D. Dissanayake, D. C. Tsang, S. Kim, H. W. Kua & K. W. Shah (2022) Preparation and thermal conductivity enhancement of a paraffin wax-based composite phase change material doped with garlic stem biochar microparticles. *Science of the Total Environment,* 827**,** 154341.

Yousef, S., J. Eimontas, N. Striūgas, S. P. Subadra & M. A. Abdelnaby (2021) Thermal degradation and pyrolysis kinetic behaviour of glass fibre-reinforced thermoplastic resin by TG-FTIR, Py-GC/MS, linear and nonlinear isoconversional models. *journal of materials research and technology,* 15**,** 5360-5374.

683 Yuan, X., T. He, H. Cao & Q. Yuan (2017) Cattle manure pyrolysis process: kinetic and thermodynamic
684 analysis with isoconversional methods. *Renewable Energy,* 107**,** 489-496.
685 Zhang, W., X. Zhang, X. Zhang, Z. Yin, Y. Liu, M. Fang, X. Wu, X. Min & Z. Huang (2019) Lauric-stearic
686 acid eutectic mixture/carbonized biomass waste corn cob composite phase change materials:
687 Preparation and thermal characterization. *Thermochimica Acta,* 674**,** 21-27.